Electrochemical Impedance Spectroscopy for the determination of oxide ion conductivity

Naeemakhtar Momin[1], J. Manjanna[1,*]

1 . Dept. of Chemistry, Rani Channamma University, Belagavi-591156, Karnataka, India
Email: jmanjanna@rediffmail.com

Received: 22.5.22, Revised: 30.6.22, Accepted: 2.7.2022

Abstract

The properties of oxide ion conductors depend upon the structure, compositions, nature of interface, dopant and defects dissemination. The electrochemical impedance spectroscopy (EIS) is emerged as strong tool for disentangling the intricacies of oxide ion conductors, and their capacities by using the different frequencies reliance for the isolations into their constituent's parts. Consequently, the electrical homogeneities in oxide ion conductors used for SOFC applications like anode/electrolyte/cathode, grain, grain boundary (GB) conductivity, area specific resistance of fuel cell and temperature coefficient of resistance can generally be examined effectively by utilizing the EIS.

Keywords: Electrochemical Impedance Spectroscopy; Solid Oxide Fuel Cells; Electrolyte; Oxide ion conductivity

Introduction

The fuel cell technology has emerged to be an alternative potential in the present energy crisis as it is capable to drench high-performance energy output of environmental benefits over other energy devices. Fuel cells as a significant part comprise customary solid oxide fuel cells (SOFCs), giving largely account to the recent innovation advancement and expected to emerge as major technological distribution for energy generation till 2030[1]. The elective procedures of determining electrical properties are impedance spectroscopy, wherein measurements are done over wide range of frequencies to characterize the different regions of the materials with respect to their relaxation time or time constant[2]. Impedance spectroscopy is moderately simple to utilize and is appropriate to a wide assortment of materials and issues. It has gone through significant advancements as of late with the accessibility of programmed gear fit for spreading over numerous times of recurrence in a solitary scope. A distant memory are the times of adjusting R and C (or L) circuits utilizing invalid strategies, where it could require a few minutes to get a particular reading. The principal reason for this review is

DOI: 10.59143/isas.jisas.1.1.CZEF7076

to show the value of impedance spectroscopy for the characterization of SOFC electrolytes[3-6]. It is quickly turning into a fundamental strategy in the advancement of novel materials for energy applications due to the fact that it empowers the by and large electrical properties of a material to be isolated into their elemental components, which can then be deliberately, considered or changed[7-10].

Electrochemical Impedance spectroscopy (ESI)

The EIS is a technique used for the electrical characterization of electroceramics. The a.c. current is applied to the sample over a wide range of frequencies to record the response of the sample[11-13]. The EIS is employed to study the properties of ionic conductors, dielectric materials, semiconductors, solar cells, fuel cells, batteries and corrosion etc. In 1967 Bauerle[14] introduced the EIS technique to determine the oxygen ion conductivity in solid electrolytes[15]. The information about the electrode process and contribution of grain and GB conductivity to the total conductivity can be obtained using the EIS technique. The parallel RC elements represent the different regions of the materials. The product of the resistance and the capacitance of the element in the region is a characteristic time constant[16]. Thus, the regions can be identified as the frequency of maximum loss (ω_{max}), with capacitance calculations using eq. (1).

$$\tau = RC \; ; \; \omega_{max} RC = 1 \qquad (1)$$

Because of the geometrical relation between the capacitance, thickness and surface area of the sample, the magnitude of the capacitance is related to the phenomenon in the sample. Typical impedance spectrum is represented as negative of the imaginary impedance component (Z'') versus real impedance (Z') and termed as Nyquist plot. The equivalent electrical circuits were used to fit the experimental data to represent the physical behavior of the materials. In mixed conductors, the probable behavior is comprised of ionic and electronic[17]. Since ions could have travelled through various components and respective impedance could be related to it. The electrical behaviors of the materials can be analyzed by plotting different plots such as complex plane impedance and capacitance, spectroscopic plots of capacitance, electric and impedance modulus. The total ionic resistance would be the sum of the grain and grain boundary resistance, if the grain and GB effects appear in impedance spectra.

The series model to the current pathway.

$$R_i = R_b + R_{gb} \qquad (2)$$

$$R_b = R_{b,i} \times R_{b,e} / R_{b,i} + R_{b,e} \quad (3)$$

$$R_{gb} = R_{gb,i} \times R_{gb,e} / R_{gb,i} + R_{gb,e} \quad (4)$$

Huggins[18] has proposed complex impedance plots of pure ionic conductors and pure electronic conductors shown below to obtain the transport number from the complex impedance plane. The plots for mixed conductors without grain and grain boundaries are also shown in Fig.1 and 2 respectively.

The ionic and electronic resistance of the material is represented by the real axis of the complex impedance spectra[19]. The resistance and transport number for ionic and mixed conductors can be calculated using the above-mentioned equation (eq. 4). For the high electron transfer number, the semi-circle arc at high frequency would be larger than at low frequency. For high ionic transport numbers, the semi-circle arc at high frequency is smaller than at low frequency[20].

The complex impedance of a sample is measured as a function of frequency and depicted in the form of Nyquist plots. Generally, the a.c impedance spectrum of solid ionic conductors shows three different contributions. The arc, at high frequencies, is attributed to grain (bulk) behavior, at intermediate frequencies, attributed to grain-boundary (GB) behavior, and at lower frequencies belongs to electrode behavior which is regarded to be more complex due to the appearance of multiple arcs. Due to different relaxation time constants for individual polarizations of conductors at a constant temperature, all the arcs will not appear simultaneously, and hence with a rise in temperature grain and GB arcs at high frequencies tend to disappear, and only total electrode contribution (arc) will be observed at high temperature[21]. The other reason for this behavior could be similar relaxation time of charge carriers inside the grain and GB, hence with the increase in temperature, the semicircle arc of grain and GB contributions were overlapped and difficult to distinguish. To distinguish the grain, GB, and electrode, contributions equivalent electrical circuit model [R(QR)(QR)] had been employed, which is shown in Fig.3. This equivalent circuit consists of the grain resistance (R_g) and two RC circuits in series for GB (R_{gb}) and the other for electrode polarization (R_e). A constant phase element (CPE= Q) is applied instead of a capacitor. This constant phase element is equivalent to the distribution of the capacitor in parallel. The element R_g, $R_{gb} \| Q$ represents the ionic conductivity through grain and grain boundary[22]. The total resistance of the electrolyte is calculated by using the eq. (5).

$$R_{total} = R_g + R_{gb} \quad (5)$$

Where R_g and R_{gb} be the grain and GB resistance, respectively

The total conductivity is obtained by using eq. (6).

$$\sigma = t/RA \quad (6)$$

where t be the thickness of the pellet, R is the resistance, and A is the total surface area.

The capacitance values were computed using the equation ωRC = 1, where ω is the angular frequency (=2πf, f is the frequency in Hz) and R is the arc magnitude. Grains have a capacitance of pF, whereas GB has a capacitance of nF [23-25].

Arrhenius equation is used to show the influence of temperature on conductivity [26] eq. (7).

$$\sigma T = A_o \exp^{\left(\frac{-E_a}{KT}\right)} \quad (7)$$

where σ, A_o, T, E_a and K are the conductivity, pre-exponential constant, temperature, activation energy, and Boltzmann constant, respectively.

As a typical case the reported oxide ion conductivity of $Ce_{1-x}La_xO_{2-\delta}$ ($0 \leq x \leq 0.1$), LDC samples were determined using EIS techniques [24]. For a.c. impedance measurement, the silver paste was applied on both sides of the LDC pellet samples and baked at 600 ºC for 1 h for electrical connection. The electrochemical impedance spectrometer (CH Instrument, Inc CHI604D USA) was used to record the Nyquist plots at different temperatures from 350 − 750 ºC in the frequency range of 1 – 10 MHz with an a.c. signal of 10 mA. The obtained data were fitted to the corresponding equivalent circuits [R(QR)(QR)] using the ZSimpWin software to obtained the polarization resistance for grain and grain boundary (GB) as shown in the below Fig. 4.

The fitting parameters of 0.5 LDC sample at 700 ℃ are given here as typical case in Table. 1.

From the above plots (Fig. 5) it has been clearly observed that, the semicircles of grain and grain GB were found to be overlapped and depressed. This depression of semicircles might be due to varying sizes and distribution of grain inside the samples. The total conductivity (σ_t) was calculated using the eq. (6). The obtained Nyquist plots of 0.05 LDC sample after fitting are shown in Fig. 5[24]. Based on the obtained results the total ionic conductivity of 0.05 LDC samples at 700 ℃ was computed using the eq. (6) and was found to be 8.32×10^{-3} S cm^{-1}. Thus, the EIS techniques provide facile route for the determination of ionic conductivities for SOFC materials. The capacitance values were found to be in the range of 10^{-12} – 10^{-8} F, which indicates the conduction process through grain and grain boundary, respectively. The work on the characterization of materials for SOFC applications has gained momentum and now it is evident that with the help of EIS an abundance of data might be

gotten. Future improvements are probably going to include the isolation and characterization resonance/relaxation phenomenon and determination of ionic and electronic components[25, 26].

Conclusions

This brief outline of electrochemical impedance spectroscopy (EIS) portraying the convenience of materials characterizations is related to energy applications. The measurement of grain and grain boundary (GB) resistance are important parameter of SOFCs electrolytes and therefore determination of ionic conductivity for SOFCs are prime concern. Thus, in this review we utilize the way that materials have quantifiable electrical properties to permit us to concentrate determination of oxide ion conductivity of the materials for SOFCs.

Acknowledgements

Authors greatly acknowledge the financial support from (i) BRNS/ DAE, Govt. of India [37 (2)/14/20/2015/BRNS] (ii) DST-FIST, Govt. of India [SR/FST/CSI-273/2016] and (iii) VGST K-FIST-Level-II and CESEM, Ministry of IT, BT and S & T, Govt. of Karnataka.

Figures:

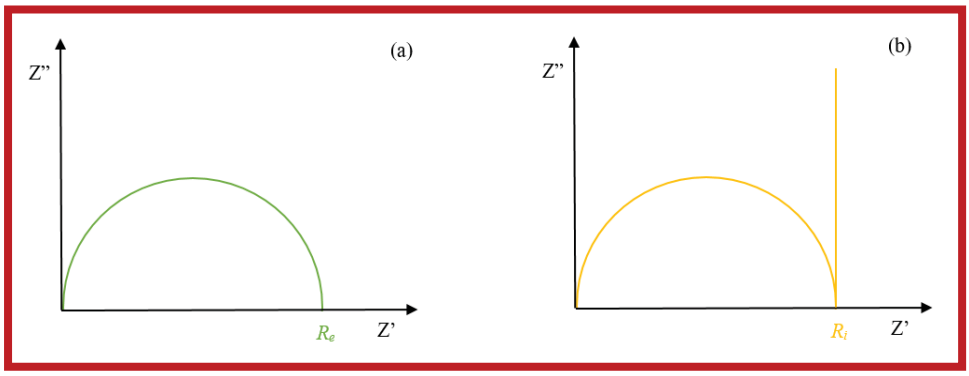

Fig. 1: Complex impedance plane of a purely electronic (a) and ionic conductor (b) [18].

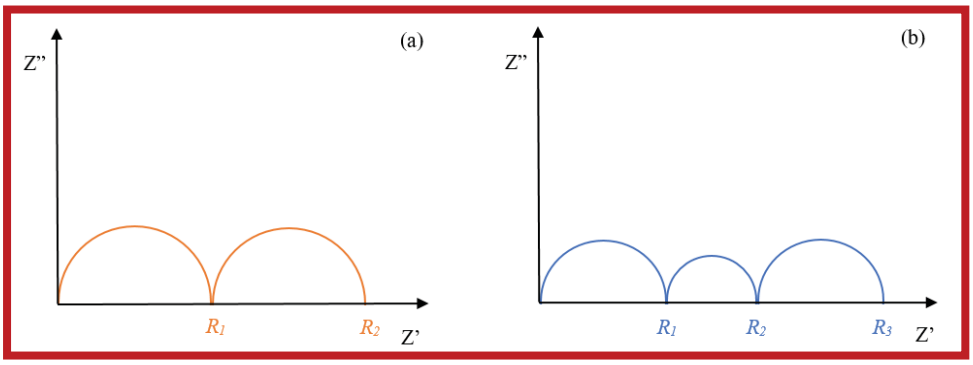

Fig. 2: Complex impedance plane of mixed conductor with 2 elements(a) and 3 elements(b).

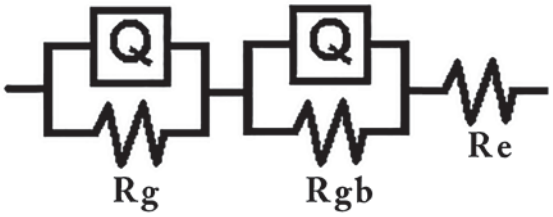

Fig. 3: electrical model used to fitting arcs [R(QR)(QR)].

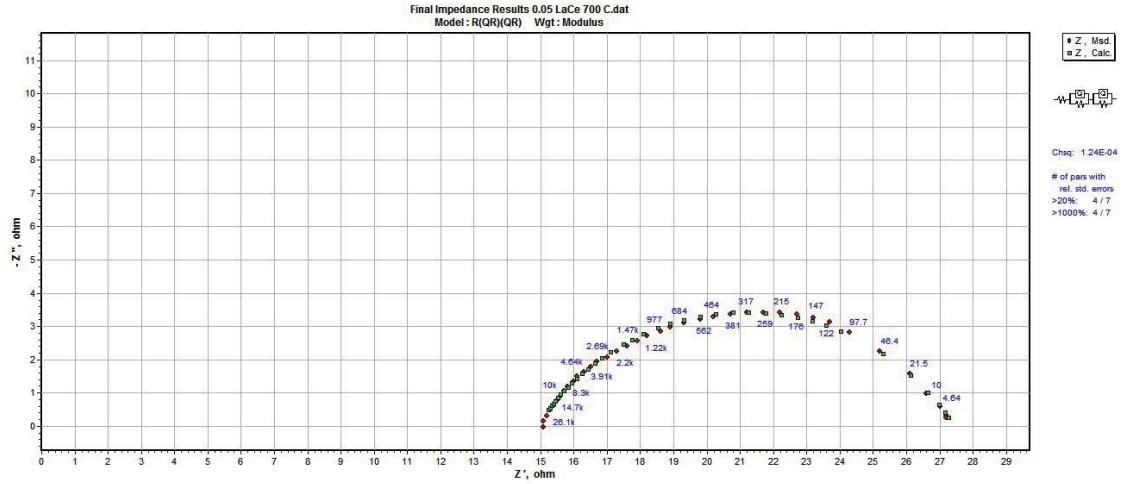

Fig. 4: Shows 0.05 LDC data fitting arcs with [R(QR)(QR)]circuit in ZSimpWin software.

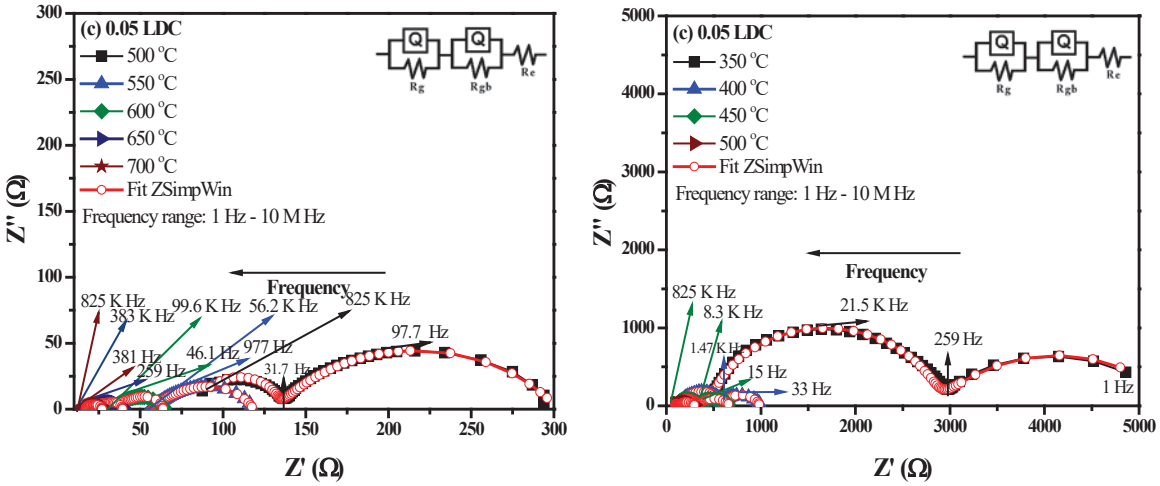

Fig. 5: Nyquist plots for 0.05 LDC measured between temperature range of 350 − 750 ºC.

Tables:

Table 1: Nature of resistances and transport numbers for electronic, ionic, and mixed conduction.

Conduction	Resistance	Electronic Transport Number t_{ele}	IonicTransport Number t_{ion}
Electronic	Re	1	0
Ionic	Ri	0	1
Mixed	Re × Ri / Re + Ri	Ri / Re	Re – Ri / Re

Table 2: EIS data analysis results of 0.05 LDC sample at 700 ℃ from ZSimpWin software

Index	Parameter	Start	End
1	R	14.9	10.81
2	Q-Yo (CPE)	0.06227	0.0006227
3	Q-n (Frequency Power)	0.8	0.6361
4	R_{gb}	12.55	12.55
5	Q-Yo (CPE)	8.97E-14	6.218E-18
6	Q-n (Frequency Power)	0.8	0.3789
7	R_g (Resistance)	0.01	4.09
Where, R is the resistance in Ω, Q-n is the frequency power in n and Q-Yo is the constant phase element (CPE) in S. s^n.			

References:

1. N. Jackson, R. Morgan, D. Brett, Fuel Cell Technology Roadmap, automotive council UK, version 1.0, 2020.
2. A. Orera, P.R. Slater, Chem. Mater., 22 (3), 675, 2010.
3. H. Yahiro, T. ohuchi, K. Eguchi, H. Arai, J. Mater. Sci., 23 (3), 1036,1988.
4. K. Eguchi, T. Setoguchi, T. Inoue, H. Arai, Solid State Ion., 52(1-3), 165, 1992.
5. J. Zhang, L. Lei, F. Zhao, F. Chen, M. Han, Electrochim. Acta., 340, 135898, 2020.
6. J. Nielsen, J. Hjelm, Electrochim. Acta. 115, 31, 2014.
7. M. Gödickemeier, D.W. Eth, Mixed Ionic Electronic Conductors for Solid Oxide Fuel Cells Table of Contents, Betrieb., 11348, 1996.
8. M. Zarabian, M. Bartolini, P. Pereira-Almao, V. Thangadurai, J. Electrochem Soc.,164(6), A1133, 2017.
9. J. Zhang, C. Lenser, N.H. Menzler, O. Guillon, , Solid State Ion., 344, 115138, 2020.
10. M. Lang, T. Franco, G. Schiller, N. Wagner, J. Appl. Electrochem., 32(8), 871, 2002.

11. J. Hjelm, M. Sø̸gaard, M. Wandel, M. Menon, M. Mogensen, A. Hagen, ECS Trans., 7(1), 1261, 2007.
12. [R.R. Mosbæk, J. Hjelm, R. Barfod, J.V.T. Høgh, P.V. Hendriksen, Proc. 10th European SOFC Forum B10, PP56, 2012.
13. A.R.C. Bredar, A.L. Chown, A.R. Burton, B.H. Farnum, ACS Appl. Energy Mater., 3(1), 66, 2020.
14. J.E. Bauerle, J. Phys.Chem. Solids., 7 (15), 2657, 1969.
15. H. Nara, T. Yokoshima, T. Osaka, Curr. Opin. Electrochem., 20, 66, 2020.
16. A. West, J. Irvine, D. Sinclair, Adv. Mate., 2(3), 132, 1990.
17. K. Kobayashi, Y. Sakka, T.S. Suzuki, J. Ceram. Soc. JPN., 124(9) 943, 2016.
18. H. Herrera Hernández, A. M. Ruiz Reynoso, J. C. Trinidad González, C. O. González Morán, J. G. Miranda Hernández, A. Mandujano Ruiz, J. Morales Hernández, R. Orozco Cruz, Electrochemical Impedance Spectroscopy, IntechOpen, ,2020.
19. M.E. sayed Ali, O.A. Abdelal, A.A. Hassan, Solid State Ion., 178, 1463, 2007.
20. J. Nielsen, J. Hjelm, Electrochim. Acta., 115, 31, 2014.
21. S. Banerjee, P.S. Devi, D. Topwal, S. Mandal, K. Menon, Adv. Funct. Mater., 17(15), 2847, 2007.
22. A. Ali, R. Raza, M. A. Rafique, B. Wang, B. Zhu, Appl. Phys. Lett., 112(4), 043902, 2018.
23. K.C. Anjaneya, G.P. Nayaka, J. Manjanna, G. Govindaraj, K.N. Ganesha, J. Alloys Compd., 578, 53, 2013.
24. N. Momin, J. Manjanna, L. D'Souza, S.T. Aruna, S. Senthil Kumar, J. Alloys Compd., 896, 163012, 2022.
25. T. hang, J. Ma, Y. Chen, L. Luo, L. Kong, S. Chan, Solid State Ion., 177 (13-14), 1227, 2006.
26. E.M. Köck, M. Kogler, B. Klötzer, M.F. Noisternig, S. Penner, ACS Appl. Mater. Interfaces., 8(25), 16428, 2016.